PHYS 798C Spring 2024
Lecture 29 Summary

Prof. Steven Anlage

I. THE CUPRATE MATERIALS

The cuprate superconductors all have one thing in common - the presence of square CuO_2 planes in their crystal structures (see Fig. 1). These materials are all insulating anti-ferromagnetic materials in the un-doped, or parent compound, state. The anti-ferromagnetism is centered in the CuO_2 planes and the Neel temperature is typically near or above room temperature. The insulating state is due in part to the strong on-site Coulomb repulsion created when additional charge carriers try to doubly occupy the Cu d-orbitals. Hence the d-electrons remain localized on each lattice site.

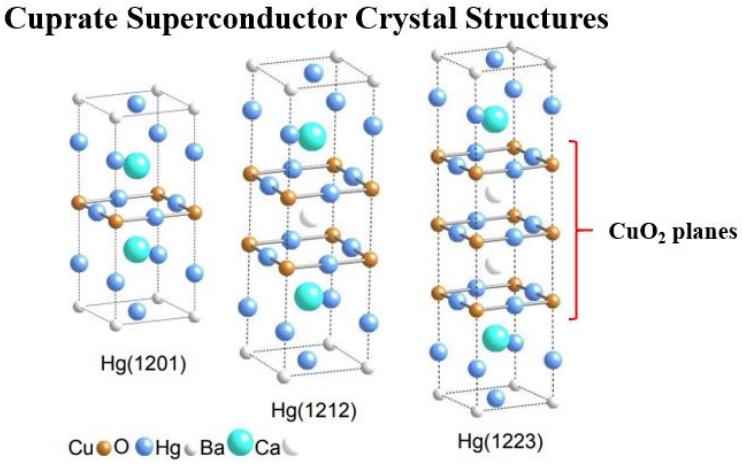

FIG. 1. Crystal structures of the Hg-based cuprate family going from 1-layer to 3-layer structures. The figures in this document come from D. J. Scalapino, "A common thread: The pairing interaction for unconventional superconductors," Rev Mod Phys 84 (4), 1383-1417 (2012); and D. J. Scalapino, "Superconductivity and Spin Fluctuations," J Low Temp Phys 117, 179-188 (1999).

Things change when the CuO_2 planes are doped with carriers, either holes or electrons. The Neel temperature drops dramatically with carrier doping, going to zero at a critical doping (see Fig. 2). Somewhere beyond this doping superconductivity appears, again localized in the CuO_2 planes. The phase diagram of the cuprates shows the temperature-doping plane and includes multiple phases and states. One of the confusing aspects of these materials is that there are many competing effects acting simultaneously, and it is difficult to unambiguously identify the precise mechanism for each observed feature. The un-doped materials can be doped with either holes or electrons, although usually not in a single material.

II. SUPERCONDUCTIVITY IN THE CUPRATES

It was demonstrated through flux quantization measurements by Colin Gough that the cuprates have paired charge carriers, giving rise to flux quantization in units of $\Phi_0 = h/2e$. It was also shown that the pairs involve a spin singlet state through measurements of the Knight shift in the superconducting state. The interaction between the electron spin $\vec{S}$ and the nuclear moment $\vec{I}$ is $\mathcal{H}_{int} \sim \vec{S} \cdot \vec{I}$, leading to the Knight shift $K(T)$ that measures the electron spin susceptibility. This is observed to go to zero in the limit of zero temperature, consistent with a spin singlet pairing state. By the way, spin-triplet paired superconductors show a much smaller Knight shift below T_c because the spin susceptibility of those pairs remains high.

A number of thermodynamic properties of the cuprates suggest that they have nodes in the superconducting energy gap on the Fermi surface. These include measurements of the magnetic pene-

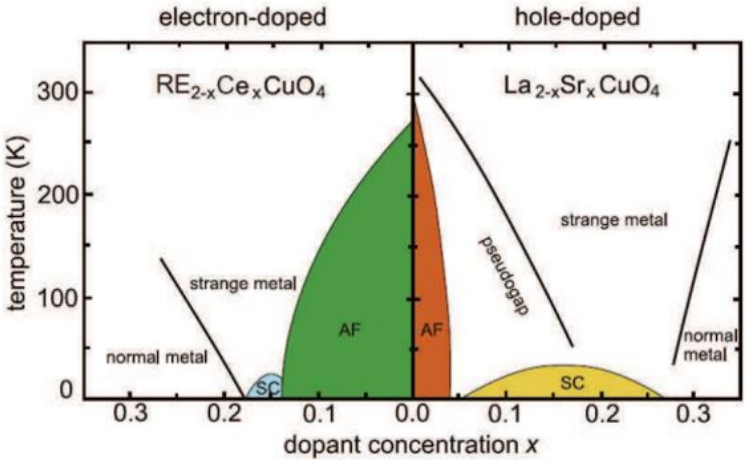

FIG. 2. Phase diagram of the electron-doped and hole-doped cuprate superconductors. Note the superconducting domes as a function of doping, characteristic of materials with competing interactions between superconductivity and other forms of long-range order.

tration depth temperature dependence at low temperatures. In conventional s-wave superconductors the penetration depth increases from its zero temperature value slowly as a function of temperature, $\lambda(T) - \lambda(0) \sim e^{-\Delta(0)/k_B T}$ for $T < T_c/3$. This activated behavior is due to the fully-gapped nature of the Fermi surface, $\Delta_{\vec{k}} \sim \Delta_0$. Nodal superconductors show a power-law temperature dependence of the penetration depth, $\lambda(T) - \lambda(0) \sim T^n$, with $n = 1$ for the cuprates. This value of n is expected for superconductors with line-nodes of the energy gap on the Fermi surface.

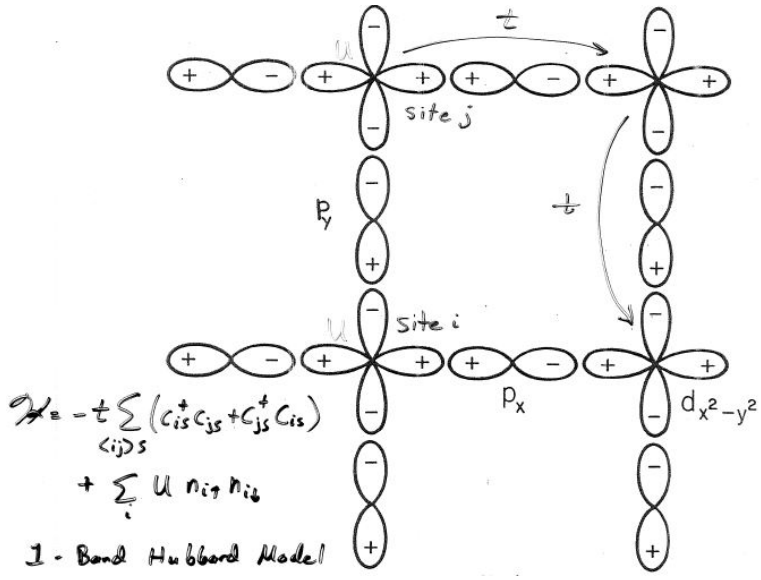

FIG. 3. Diagram of orbitals in a single CuO_2 plane, along with the 1-band Hubbard model Hamiltonian.

III. PAIRING MECHANISM IN THE CUPRATES

It is commonly believed that an electronic pairing mechanism, as opposed to an electron-phonon mechanism, is responsible for superconductivity in the cuprates. A simple model of electron transport in the CuO_2 planes is the Hubbard model. In the simple 1-band Hubbard model we treat the Cu $d_{x^2-y^2}$ orbitals as being in a square lattice, with lobes joined to each other through O p_x and p_y orbitals (see Fig. 3). A charge carrier can hop from one Cu to another with transfer energy t. If two charge carriers occupy the same Cu at once, there is a large Coulomb repulsion price $U >> t$. The simple 1-band

Hubbard Hamiltonian is,

$$\mathcal{H} = -\sum_{\langle ij\rangle s} t(c_{is}^{+}c_{js} + c_{js}^{+}c_{is}) + \sum_{i} U n_{i,\uparrow} n_{i,\downarrow}$$

where $n_{is} = c_{i,s}^{+}c_{is}$ is the number operator on site i for spin s, and the notation $\langle ij\rangle$ refers to sites i and j that are nearest neighbors in the square lattice. Here t is the effective one-electron transfer energy, and U is the on-site Coulomb repulsion.

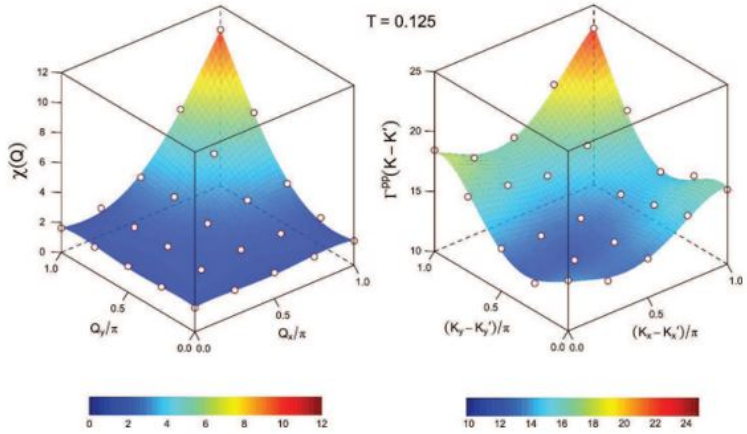

FIG. 4. (Left) Spin susceptibility $\chi(\vec{k},\vec{k}')$ of charge carriers in the CuO_2 plane shown in one quarter of the Brilloiun zone. (Right) Pairing interaction $V(\vec{k}-\vec{k}')$ in a quarter of the Brillouin zone.

At half-filling of the band there is one electron per Cu site and the ground state shows anti-ferromagnetic long-range order in a certain range of U/t (see for example arXiv:1505.02290, published as Phys. Rev. X 5, 041041 (2015)). The nature of this antiferromagnetic ground state is thought by some to be an spin-liquid state, rather than a static ordered array of spins. It is thought by some theorists that away from half-filling, the Hubbard model is unstable to correlations that resemble superconductivity in the low temperature limit.

How might superconductivity come about in the CuO_2 planes? Berk and Schrieffer (Berk, N. F., and J. R. Schrieffer, Phys. Rev. Lett. 17, 433 (1966)) calculated a pairing interaction associated with anti-ferromagnetic spin fluctuations of the form $V_{\vec{k}\vec{k}'} = \frac{3}{2}U^2\chi(\vec{k}-\vec{k}')$, where $\chi(\vec{k}-\vec{k}')$ is the spin susceptibility at the difference wavenumber. They were interested in understanding why spin fluctuations suppress the T_c of s-wave superconducting materials such as Pd (4d transition metal just below Ni in the periodic table). In the cuprates, calculations show that the spin susceptibility is strongly peaked at the corners of the Brillouin zone, (π,π), $(\pi,-\pi)$, $(-\pi,\pi)$, and $(-\pi,-\pi)$ (see Fig. 4). However, the spin susceptibility, and the resulting pairing interaction, are both strictly positive. This would seem to preclude the possibility of superconductivity. Indeed in the s-wave (zero orbital angular momentum pairing state) with electron momenta $\vec{k}$, $-\vec{k}$ there is no superconductivity.

To understand how superconductivity comes about, it is useful to Fourier transform the pairing interaction into real space, $V(\vec{r}) = \int e^{i\vec{q}\cdot\vec{r}}V(\vec{q})d^3q$. Figure 5 shows a very strong on-site repulsion, signified by the large positive (red) value of $V(l_x = l_y = 0)$. On the other hand, there are negative values (blue) for the pairing interaction in real space, at the nearest neighbor locations in the l_x and l_y directions. This suggests that the charge carriers will avoid double occupation of a site, and preferentially choose nearest neighbor sites that are in the directions of the oxygen atoms in the CuO_2 planes. This can be accomplished if the Cooper pairs go into an $\ell > 0$ orbital angular momentum state.

Now look at the BCS gap equation, $\Delta_{\vec{k}} = -\sum_{\vec{k}'} V_{\vec{k},\vec{k}'} \frac{\Delta_{\vec{k}'}}{2\sqrt{\xi_{\vec{k}'}^2+\Delta_{\vec{k}'}^2}}$. Recall that $V_{\vec{k},\vec{k}'}$ is large and positive and peaked in value at the corners of the Brilloiun zone. To take advantage of the large values, the system has to change the sign of the gap $\Delta_{\vec{k}}$ for regions on opposite sides of the Fermi surface that differ in momentum by $(\pm\pi,\pm\pi)$ (see Fig. 6). A gap function with $d_{x^2-y^2}$ symmetry gives a self-consistent solution to the gap equation, and has the form $\Delta_{\vec{k}} = \Delta_{Max}(\cos(k_x a) - \cos(k_y a))$, where a is the lattice parameter of the CuO_2 planes. In this case the two charge carriers avoid the strong on-site repulsion and go into an $\ell = 2$ orbital angular momentum state. The nodes (or zeros) of this gap function point in the

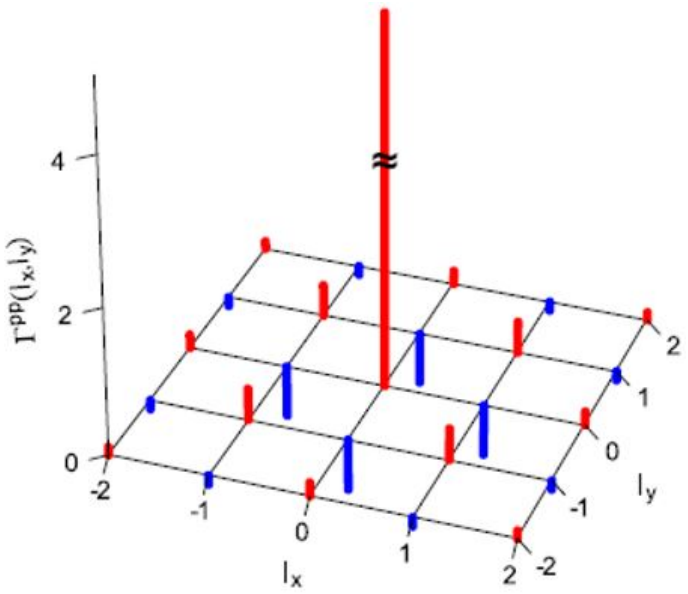

FIG. 5. Fourier transform of anti-ferromagnetic spin fluctuation pairing interaction $V(\vec{r})$ into real space (l_x, l_y). Note the large positive spike at $(l_x, l_y) = (0, 0)$

diagonal directions in real space where the short range $V(\vec{r})$ is positive. There is experimental evidence from angular resolved photoemission spectroscopy, and from several types of tunneling experiments, that this order parameter symmetry is dominant in the cuprate superconductors.

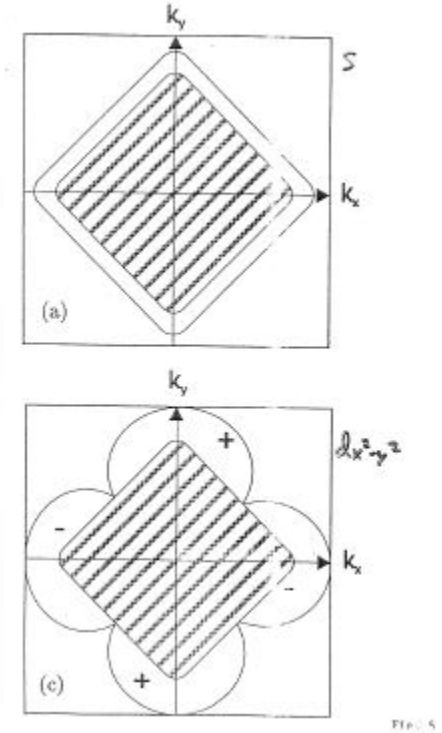

FIG. 6. Gap functions on the Fermi surface of a cuprate superconductor. (a) Upper plot shows an isotropic s-wave gap. (c) Lower plot shows the $d_{x^2-y^2}$ gap function over the Fermi surface.

IV. PROXIMITY EFFECT PHYSICS

When a superconductor and normal metal are in good electrical contact, there can be superconducting pairing correlations that diffuse into the normal metal, and quasiparticle excitaitons that diffuse into the superconductor. Using the real-space generalizaitons of BCS theory (see Lecture 14 and the book by P. G. de Gennes, *Superconductivity of Metals and Alloys*) one finds that the order parameter can be approximately factored as $\Delta(\vec{r}) = g(\vec{r})F(\vec{r})$, where $g(\vec{r})$ is the effective pairing interaction and $F(\vec{r})$ is the pair correlation function (in the normal metal), or the condensate amplitude (in the superconductor). At the S/N interface there is a suppression of $F(\vec{r})$ in the superconductor, resulting in a finite extrapolation length b, as discussed previously in the context of Ginzburg-Landau theory (Lecture 15). In general there is a discontinuity in $F(\vec{r})$ at the S/N interface, and an exponential decrease in the normal metal, $F_N(x) \sim e^{-x/\xi_N}$ (see Fig. 7 and slides on the class website). The suppression in the superconductor occurs over a length scale of order $\xi_S = \frac{\hbar v_F}{\pi\Delta}$, and the decay length scale in the (clean) normal metal is $\xi_N = \frac{\hbar v_{FN}}{k_B T}$. Note that these length scales have rather different temperature dependences, with ξ_N growing upon decreasing temperature, suggesting that superconducting pair correlations can reach deep into the normal metal at low temperatures.

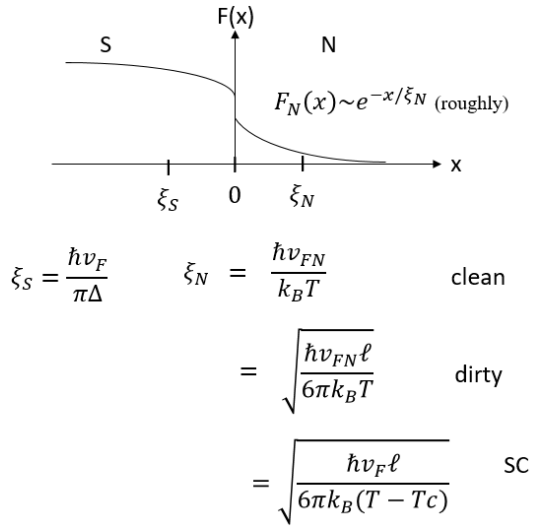

FIG. 7. Schematic variation of the pair correlation function $F(x)$ as a function of position x near the superconductor / normal boundary at $x = 0$. Expressions for the correlation lengths in the superconductor and normal metal, in the clean and dirty limits, are also given. From Prof. Dale van Harlingen, UIUC.

A number of physical consequences result from the proximity effect. These include,

1. The transition temperature T_{cNS} of a bilayer of finite-thickness S and N layers will depend on their thicknesses d_S and d_N. See Fig. 8. Note that the T_{cNS} as a function of d_N saturates as long as the superconductor thickness satisfies $d_S > \xi_S$.

2. The proximity-coupled normal metal will develop superconductor-like screening of electromagnetic fields and show reduced surface resistance losses. See the slides on the class website.

3. A S/N/S trilayer sandwich can display Josephson coupling between the two superconducting banks, provided the N-layer thickness is not too great.

V. ANDREEV SCATTERING

A. F. Andreev was considering the problem heat transport through an N/S interface in the intermediate state at low temperatures. It was noted that the heat current carried by normal electrons with energies E less than the superconducting gap Δ was reflected at the interface, while the electrical current proceeded through without interruption. Andreev proposed a mechanism to account for this behavior, now known as Andreev scattering. The process is illustrated in Fig. 9. The upper part of the figure shows the situation in k-space. If the quasiparticle energy $E > \Delta$ there are single-particle states available in the

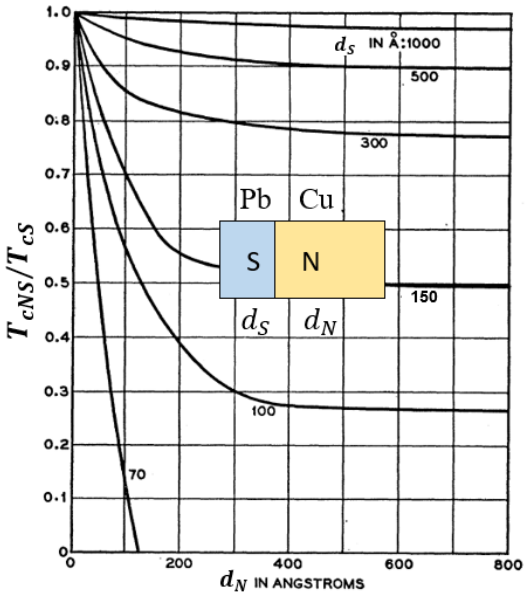

FIG. 8. Superconducting transition temperature of S/N proximity bilayer for the Pb/Cu pair, as a function of normal metal thickness d_N with superconducting layer thickness d_S as a parameter. From N. R. Werthamer, "Theory of the Superconducting Transition Temperature and Energy Gap Function of Superposed Metal Films," Phys Rev 132 (6), 2440 (1963).

superconductor, so the quasiparticle can enter with some finite probability. However, if the quasiparticle energy $E < \Delta$ there are no single-particle states available in the superconductor, so the quasiparticle cannot enter. In this case, Andreev proposed that a quasi-hole is *retro-reflected* (not specularly reflected) from the interface, and a Cooper pair is transmitted into the superconductor. These processes occur so as to conserve energy, charge and momentum. The net result in real space is shown in the lower half of Fig. 9. Since the Cooper pairs cannot carry entropy, the heat current carried by the sub-gap electrons will be reflected at the interface. However, the electrical current is conserved as there is a net flow of two charges to the right in both metals. Note that this is one process by which normal electrical current is converted into supercurrent at an N/S interface, and does not involve dissipation.

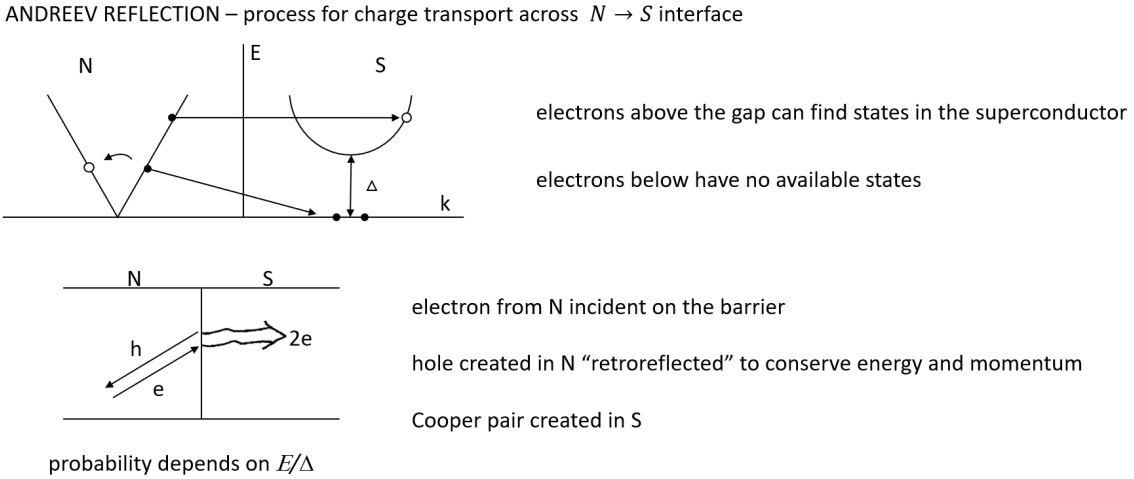

FIG. 9. Schematic illustration of Andreev scattering for electrical transport from a normal metal into a superconductor with gap Δ. Original paper: A. F. Andreev, "The Thermal Conductivity of the Intermediate State in Superconductors," J. Exp. Theor. Phys. 19 (5), 1228 (1964). Figure from Prof. Dale van Harlingen, UIUC.

Another measureable consequence of Andreev scattering is seen in point contact spectroscopy. A point contact (or Sharvin contact) between a normal metal and a superconductor can show a doubling of conductance for bias voltages less than than the superconducting gap Δ. This can be used to measure the energy gap as a function of temperture, for example. The Blonder-Tinkham-Klapwijk (BTK) model

makes predictions for the conductance of the point contact as a function of voltage bias, and includes the effect of a narrow barrier at the S/N interface.

The Andreev scattering process is very helpful for understanding the microscopics of the Josephson effect in SNS junctions. In particular an elecron-hole pair can coherently scatter between the two S/N interfaces in the junction, leading to "Andreev bound states" with energies within the superconducitng gap. The energies of these states depend on the GIPD between the superconductors. The existence of these bound states also changes the current-phase relation for the junction.